Coexistence of melted and ferroelectric states in sodium nitrite within mesoporous sieves

Cheng Tien,[1] E. V. Charnaya,[1,2] M. K. Lee,[1] S. V. Baryshnikov,[3] S. Y. Sun,[1] D. Michel,[4] and W. Böhlmann[4]
[1]*Department of Physics, National Cheng Kung University, Tainan, 70101 Taiwan*
[2]*Institute of Physics, St. Petersburg State University, St. Petersburg, Petrodvorets, 198504 Russia*
[3]*Blagoveschensk State Pedagogical University, Blagoveschensk, 675002 Russia*
[4]*Faculty of Physics and Geosciences, University of Leipzig, Leipzig, D-04103 Germany*
(Received 5 May 2005; revised manuscript received 27 July 2005; published 12 September 2005)

Results of NMR studies of ^{23}Na in $NaNO_2$ confined within molecular sieves MCM-41 with pore size 37 and 20Å and SBA-15 with pore size 52Å are presented. ^{23}Na spin-lattice relaxation and line shape were measured in a large temperature range up to 535 K covering the bulk ferroelectric phase transition point. It is shown that confined $NaNO_2$ below the bulk sodium nitrite melting point consists of two parts with relaxation times which differ by two orders in magnitude. A portion of $NaNO_2$ exhibits bulk-like properties with the ferroelectric phase transition in the vicinity of the bulk transition temperature. The bulk-like $NaNO_2$ prevails below and near the ferroelectric phase transition and its amount decreases strongly when temperature approaches the bulk melting point. Fast nuclear relaxation in another portion of confined $NaNO_2$ revealed very high molecular mobility. This portion increases with increasing temperature and dominates above 510 K. It was suggested that fast relaxation corresponds to the melted or premelted state of confined $NaNO_2$ caused by confinement. Temperature evolution of the ^{23}Na NMR line confirms such a suggestion. The amount of $NaNO_2$ which possesses high molecular mobility depends on pore size and is maximal for the MCM-41 porous matrix with 20Å pore size. The correlation time of electric field gradient fluctuations was found for this part to be similar to those in viscous liquids with the activation energy of about 0.42 eV.

DOI: 10.1103/PhysRevB.72.104105 PACS number(s): 64.70.Nd, 64.70.Dv, 76.60.−k, 77.84.Lf

I. INTRODUCTION

A great deal of attention was recently focused on size effects in low-dimensional ferroelectric structures in view of their various prospective applications in microelectronics, engineering, and technology.[1] In particular, studies of small ferroelectric particles revealed pronounced alterations in their features compared to bulk (see Refs. 2–7 and references therein). The most noticeable size effects were observed near the ferroelectric phase transitions. It was found that the temperatures of the phase transitions generally shift with respect to those in bulk, the phase transitions diffuse, and the ferroelectricity can be destroyed at some critical particle dimensions. Spontaneous polarization, domain structure, and susceptibility were also reported to be affected. Most of such studies were carried out for ensembles of ferroelectric nanoparticles in powder or on substrates. On the other hand, small ferroelectric particles can be produced by embedding ferroelectric materials into nanoporous matrices (see, for instance, Refs. 8 and 9) along with conventional methods of small particle fabrication. In such a case the particle dimensions are controlled by pore sizes and the ferroelectric particles form a structure whose geometry is governed by the geometry of the pore network. Confined geometry has some advantages since it prevents particle conglutination, regulates interparticle distances, and screens particles to a certain degree from a destructive influence of the surrounding environment. Confinement conditions were used to study size effects on different phase transitions including the melting and crystallization (see Refs. 10–13 and references therein), superconductive (see Ref. 14 and references therein), and superfluid transitions (see Refs. 15 and 16 and references therein), glass formation (see Refs. 17 and 18 and references therein), and phase separation in liquids (see Ref. 19 and references therein).

In the present paper we report results of detailed NMR studies of ^{23}Na in $NaNO_2$ (sodium nitrite) particles embedded into MCM-41 with two different pore sizes and SBA-15 mesoporous sieves within a large temperature range up to 535 K. Bulk $NaNO_2$ undergoes two successive structural transitions from a ferroelectric to an incommensurate antiferroelectric phase and to a paraelectric phase at about 437 K and 438 K, respectively.[20] The melting point of bulk $NaNO_2$ is 544 K. The rather close temperatures of the structural and melting phase transitions in bulk sodium nitrite suggest that interplay between these two transitions might become noticeable upon decreasing particle sizes taking into account possible lowering and broadening of the freezing and melting phase transitions.[10]

II. EXPERIMENT

Two kinds of MCM-41 molecular sieves were synthesized with a typical pore size of 37 and 20 Å found by electron microscopy. The calculated BET surfaces were 984 and 660 $m^2\,g^{-1}$, respectively. The synthesis of SBA-15 was performed using a method described in Ref. 21. The pore size in the obtained SBA-15 was estimated using nitrogen adsorption-desorption isotherms as 52Å. The calculated BET surface was 764 $m^2\,g^{-1}$. $NaNO_2$ was embedded into MCM-41 with 37 and 20 Å pores (samples 1 and 2, respectively) and into SBA-15 (sample 3) sieves in melted state. After cooling the samples, the pellets were pressed under a pressure of 8000 $kg\,cm^{-2}$ and then sealed into pumped quartz tubes to prevent water absorption.

 ©2005 The American Physical Society

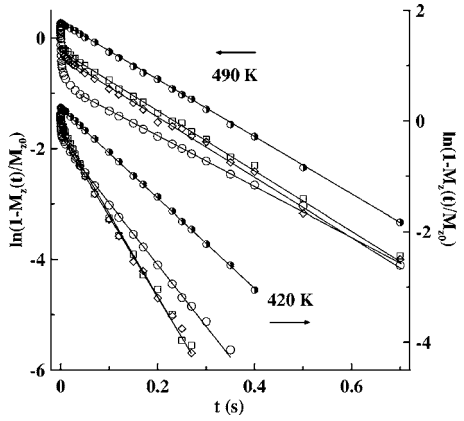

FIG. 1. ^{23}Na magnetization restoration in semi-logarithmic scale for $NaNO_2$ within mesoporous sieves measured at 420 and 490 K upon cooling. Squares, circles, and diamonds correspond to samples 1, 2, and 3, respectively. Straight lines are guides for the eye. Semi-closed circles show magnetization restoration in powder $NaNO_2$ at the same temperatures.

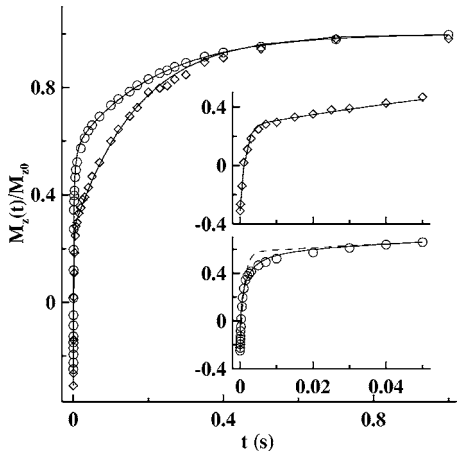

FIG. 2. ^{23}Na magnetization restoration at 490 K in sample 2 (circles) and in sample 3 (diamonds). The insets show the restoration curves at short times. Solid lines are fitting results as described in the text. The dashed line shows fitting for sample 2 when $\alpha=1$ in relationship 2.

X-ray patterns of the pellets obtained showed only very weak narrow lines from bulk $NaNO_2$. The total amount of bulk compounds was less than $\frac{1}{100}$ of the total $NaNO_2$ amount used for sample preparation and could not influence the experimental results.

^{23}Na NMR measurements for confined sodium nitrite were carried out using a Bruker Avance400 NMR pulse spectrometer operating at a Larmor frequency of 105.8 MHz (in magnetic field 9.4 T) within a range from room temperature to 535 K upon warming and cooling. For comparison, a $NaNO_2$ powder sample was also studied. Accuracy of temperature stabilization during measurements was better than 0.5 K.

The static ^{23}Na (spin $I=3/2$) NMR spectrum for bulk polycrystalline sodium nitrite shows predominantly the central $1/2 \leftrightarrow -1/2$ transition broadened by the second-order quadrupole interaction.[22] Our measurements showed that the spectra for confined $NaNO_2$ at room temperature also consisted of a single line. The restoration of the transverse magnetization corresponding to the ^{23}Na line was observed with the inversion recovery technique. The relaxation measurements were chosen because of their high sensitivity to the ferroelectric phase transition and lattice dynamics in bulk $NaNO_2$ (see Ref. 23 and references therein). In addition, the line shape was also measured. The ^{23}Na line position was referenced to a 1 M aqueous NaCl solution.

III. EXPERIMENTAL RESULTS

Measurements of the ^{23}Na NMR line restoration after a 180° pulse have shown that the recovery process for confined sodium nitrite in all samples under study cannot be described by a single exponential in contrast to bulk powder $NaNO_2$.[22] The relaxation curves in logarithmic scale for the samples under study at 490 and 420 K measured upon warming and upon cooling, respectively, are plotted in Fig. 1 as an example. They consist of two well-separated parts with quite distinctive relaxation rates. At longer time, relaxation is exponential since the restoration curves in logarithmic scale can be fitted with straight lines as in bulk (Fig. 1). For comparison, relaxation in bulk powder $NaNO_2$ at the same temperatures is also shown in Fig. 1. The similarity of the slopes of relaxation curves at longer times for confined sodium nitrite to those for bulk $NaNO_2$ is noteworthy and indicates similar relaxation rates. Spin relaxation at shorter times is much faster. This is clearly seen from Fig. 1 and also from relaxation curves in linear scale shown in Fig. 2. The shorter time part can be quite well fitted with single exponentials for samples 1 and 3 (Fig. 2). However, for sample 2, where the portion of faster relaxation is larger, the single exponential gives only a rough approximation and the stretched exponential fit is more accurate (Fig. 2). Thus, the total normalized nuclear magnetization $M_z(t)/M_{z0}$ restoration curve can be very well fitted with a following relationship,

$$1-\frac{M_z(t)}{M_{z0}}=b\left[(1-a)\exp(-t\cdot R_{\mathrm{slow}})+a\exp(-t\cdot R_{\mathrm{fast}})^{\alpha}\right], \tag{1}$$

where 1-b is the intensity of NMR signal immediately after magnetization inversion; R_{slow} and R_{fast} are relaxation rates corresponding to slower and faster relaxation components, respectively; a is the proportion of the faster component; and α is equal to 1 for samples 1 and 3. For sample 2 the stretched exponent α varies from 0.6 to 0.8 depending on temperature. Examples of the fit results are depicted in Fig. 2. The temperature dependencies of the relaxation rates and of the portion of the faster component for confined $NaNO_2$ in mesoporous sieves are shown in Figs. 3–5.

The ^{23}Na NMR line also depended strongly on temperature in all samples under study. Temperature evolution of the ^{23}Na NMR line in sample 2 is shown in Fig. 6 as an example. Below and near the ferroelectric phase transition in bulk, the line is rather broad and Gaussian. At higher temperatures it can be represented as a sum of two lines with slightly different chemical shifts and becomes narrow and Lorentzian at

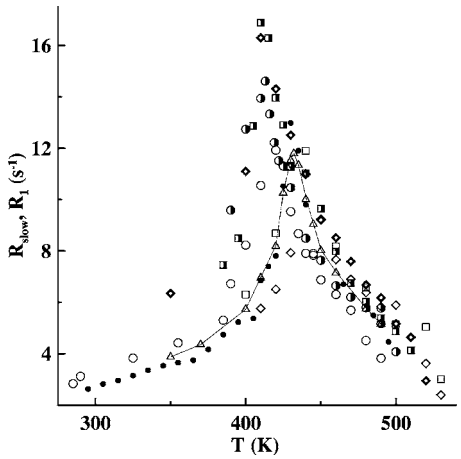

FIG. 3. Temperature dependencies of R_{slow} for confined sodium nitrite and of R_1 in bulk powder $NaNO_2$. Squares, circles, diamonds, and triangles correspond to samples 1, 2, 3, and bulk, respectively. Open symbols—warming, semi-closed symbols—cooling. Closed circles mark experimental results in sample 2 upon another warming. Solid line is a guide for the eye to clarify the R_1 versus temperature dependence in bulk.

530 K. For comparison, the ^{23}Na NMR line in bulk powder $NaNO_2$ is also shown in Fig. 6.

IV. DISCUSSION

Two well-separated stages in longitudinal magnetization relaxation and the transformation of the NMR line suggest a division of the confined sodium nitrite into two parts with different features, their relative amounts depending on temperature. The relaxation rates R_{slow} and R_{fast} corresponding to these parts differ by about two orders in magnitude. The relaxation rate of the slower component is very similar to the spin-lattice relaxation rate in bulk powder $NaNO_2$ as was already mentioned in Sec. III. The recovery curves obtained by us for bulk can be well fitted with a single exponential.

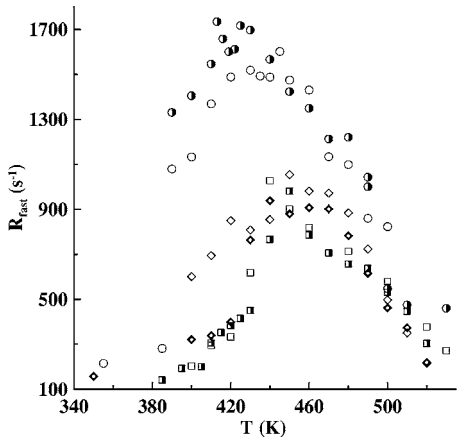

FIG. 4. Temperature dependencies of R_{fast} for $NaNO_2$ in mesoporous sieves. Squares, circles, and diamonds correspond to samples 1, 2, and 3, respectively. Open symbols—warming, semi-closed symbols—cooling.

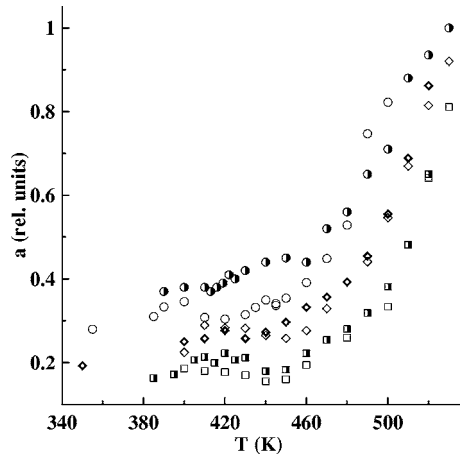

FIG. 5. Temperature dependencies of the portion a of confined $NaNO_2$ showing fast relaxation. Squares, circles, and diamonds correspond to samples 1, 2, and 3, respectively. Open symbols—warming, semi-closed symbols—scooling.

The single exponential recovery was repeatedly observed for powder $NaNO_2$ (see Ref. 22 and references therein) and agrees with theoretical predictions for quadrupole relaxation in polycrystalline samples.[24] Thus, relaxation in powder $NaNO_2$ can be characterized by a spin-lattice relaxation rate denoted here as R_1. The temperature dependence of R_1 is also shown in Fig. 3.

Both R_{slow} and R_1 show a noticeable peak near the temperature of the ferroelectric phase transition in bulk $NaNO_2$. It was shown[25] that the structural transitions in bulk sodium nitrite are related to dynamics of the NO_2 groups. At low temperature, the NO_2 groups are aligned in the bc plane of the orthorhombic unit cell and their electric dipole moments are pointed along the polar axis b. The transition from the ferroelectric phase occurs due to progressive reversal of the NO_2 dipole moments by rotation about the c axis[26] so that they are oriented with equal probability along the two directions of the b axis in the paraphase. The reorientation motion of the NO_2 groups contributes to spin-lattice relaxation of Na

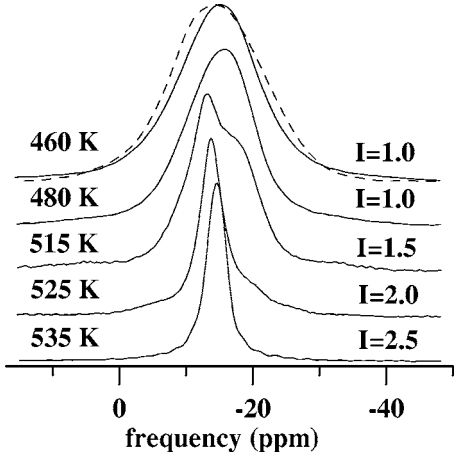

FIG. 6. ^{23}Na NMR line for sample 2 at various temperatures upon warming. Integral intensity I of lines is shown on the right. The dashed curve shows ^{23}Na NMR line in bulk $NaNO_2$ at 460 K.

nuclei. Numerous experimental studies of spin relaxation in single crystalline and polycrystalline $NaNO_2$ exhibited a relaxation rate maximum just at the ferroelectric critical point (see Refs. 22 and 23 and references therein). The relaxation enhancement near the ferroelectric phase transition was ascribed to long-wavelength fluctuations of the order parameter (electric polarization) caused by the reorientations of the NO_2 groups.[27] Note, however, that later another theoretical model was suggested that emphasized the role of thermally activated random NO_2 group flips.[23]

The fact that the spin-lattice relaxation rate for ^{23}Na in $NaNO_2$ goes through maximum just at the ferroelectric phase transition provides a convenient method of determining the critical temperature T_c which seems especially suitable for $NaNO_2$ embedded into nanoporous matrices. One can see in Fig. 2 that the portion of confined $NaNO_2$, which relaxes relatively slowly, manifests a very clear ferroelectric phase transition and thus it has bulk-like properties. Moreover, the relaxation rate peak is even more pronounced for this portion of confined $NaNO_2$ which can be related with increased role of critical fluctuations under confinement.

One can see from Fig. 3 that the relaxation peak for the slowly relaxing portion of confined $NaNO_2$ is slightly shifted along the temperature axis compared to bulk. When relaxation was observed upon warming up to about 530 K and then upon successive cooling down, the peak position upon cooling was repeatedly shifted to low temperatures compared to that found upon warming. However, our measurements showed that when we stop cooling at about 400 K and warm the samples once more, the peak position coincided with that upon cooling. This proves that the difference in peak positions upon consecutive warming and cooling is not related to a thermal hysteresis at the phase transition. The reasons for such a pseudo-hysteretic feature are not clear yet and have to be studied. Besides, we observed slight shifts in the peak position upon recurring warming-cooling thermocycles. An example in shown in Fig. 3. Note that we did not observe any regular dependence of the shift in the peak position for confined $NaNO_2$ compared to bulk on pore size (Fig. 3). The total amount of the confined sodium nitrite portion with bulk-like features dominates at temperatures near and below the ferroelectric phase transition and gradually decreases with increasing temperature (Fig. 5).

The second, faster relaxing part of the confined substance possesses very short relaxation times (Fig. 4). Its portion at a particular temperature differs noticeably for different samples and is maximal for the MCM-41 sample with 20 Å pores. Above 510 K the faster relaxing part prevails for all samples under study. Upon consecutive cooling its portion decreases in a rather reversible manner. Since the amount of faster relaxing component increases with increasing temperature, it cannot be caused by residual absorbed water. On the other hand, because of reproducible behavior upon warming and cooling, the second component cannot be explained by formation of some other chemical compounds.

Large values of R_{fast} similar to those of ^{23}Na in viscous liquids[28] show fast molecular mobility for a portion of $NaNO_2$ within molecular sieves. In this case nuclear quadrupole spin relaxation should be treated within the framework of the electric field gradient correlation function formalism.[29] For spin $I=3/2$ the longitudinal magnetization approaches its equilibrium value biexponentially,[30]

$$\frac{M(t)}{M_0} = 1 - b\left[\frac{4}{5}\exp\left(-2\left(\frac{eQ}{\hbar}\right)^2 J_{-22}(2\omega_0)t\right) + \frac{1}{5}\exp\left(2\left(\frac{eQ}{\hbar}\right)^2 J_{-11}(\omega_0)t\right)\right], \quad (2)$$

where e is the electron charge, ω_0 is the Larmor frequency, Q is the nuclear quadrupole moment and $J_{-ii}(\omega)$ are the spectral densities of the electric field gradient correlation function at the nuclear site. Assuming that the correlation function is represented by $\exp(-t/\tau_c)$ (Ref. 29) (τ_c is the correlation time of electric field gradient fluctuations), we can reduce the exponents in Eq. (2) to $-2\pi^2(C_q)^2\tau_c t/5(1+k^2\omega_0{}^2\tau_c{}^2)$, where $k=1$, 2 and C_q is the effective quadrupole coupling constant. For fast molecular mobility in the extreme narrowing limit,[30] when $\omega_0\tau_c \ll 1$, quadrupolar relaxation is single exponential with a relaxation rate $2\pi^2(C_q)^2\tau_c/5$. However, its actual behavior quite resembles a single exponential even outside of the extreme narrowing approximation as was shown in Ref. 31. It justifies the use of a single exponential characterized by R_{fast} to fit faster relaxation. The fact that fast relaxation in sample 2 is described by a stretched exponential is probably caused by disorder under confinement conditions leading to deviations of correlation time and spin relaxation rate in different points of the sample volumes from the average magnitudes. The stretched exponent α serves as a measure of the disorder. Therefore, the fitting results show that the disorder is more pronounced for the sample with the smallest pore size.

The correlation time τ_c of electric field gradient fluctuations on nuclear sites at various temperatures can be then estimated by matching relationship 2 with the second term in the right part of relationship 1. According to relationship 2, the highest relaxation rate is achieved approximately at $\tau_c\omega_o \cong 0.55$ or $\tau_c \cong 8.3\times10^{-10}$ s. This condition corresponds to the maximum of R_{fast} in Fig. 4 and makes it possible to find the quadrupole coupling constant C_q. For sample 2 the calculated quadrupole constant was found to be $C_q = 0.96$ MHz and $C_q = 0.60$ MHz for samples 1 and 3. Both values are close to the bulk $NaNO_2$ quadrupole coupling constant equal to 1.1 MHz.[22,32] Temperature dependencies of the correlation time in the samples under study are shown in Fig. 7. Variations of τ_c with temperature agree with the Arrhenius equation $\tau_c = \tau_0\exp(E_a/k_BT)$ where E_a is an activation energy as is seen from a straight line fit for sample 2 in Fig. 7, which corresponds to $E_a = 0.42$ eV. Figure 7 shows that the activation energy is nearly the same for two other samples. The estimate obtained for E_a is similar to activation energy values found for diffusion in melts.[33]

The above estimates for the correlation time are typical for viscous liquids (see, for instance, Refs. 28, 34, and 35). It suggests that the short relaxation time could be the relaxation of the melted part of confined $NaNO_2$. The increase in the portion of the fast relaxing component with increasing temperature (Fig. 5) agrees with such suggestion. A reduction of the melting temperatures for confined $NaNO_2$ compared to bulk can be related with the thermodynamic size effects on

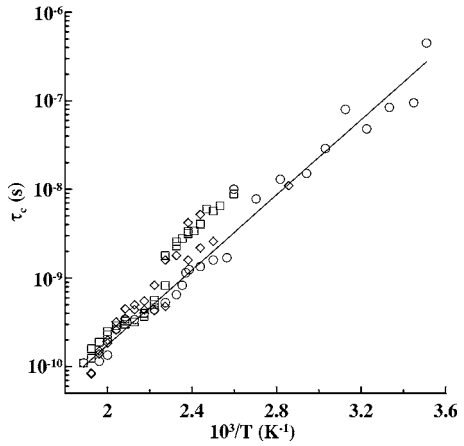

FIG. 7. Temperature dependencies of the correlation time τ_c of electric field gradients on the sodium site in the melted part of confined sodium nitrite obtained upon warming-cooling cycles. Squares, circles, and diamonds correspond to samples 1, 2, and 3, respectively. The straight line is a least-squares fit for sample 2.

the melting and freezing phase transition (see Ref. 10 and references therein). However, the increase in the relaxation rate can be related as well with fast localized molecular mobility, for instance, with rapid jumps of the NO_2 groups. In any case, the short relaxation component indicates the existence of some kind of melted or premelted state of confined $NaNO_2$ whose portion increases when temperature approaches the bulk melting point.

Thus, our NMR studies show that, below the melting point of bulk $NaNO_2$, sodium nitrite confined within molecular sieves occurs simultaneously in two states: a bulk-like one with the clear ferroelectric phase transition and a melted or premelted one with the liquid-like correlation time of molecular jumps. Temperature evolution of the ^{23}Na NMR line (Fig. 6) is in agreement with such a conclusion. In fact, the line shape at lower temperatures is mainly caused by the bulk-like portion of confined $NaNO_2$, the linewidth being similar to that in bulk. At higher temperatures when the portion of melted $NaNO_2$ gradually increases, the NMR line consists of two overlapped lines arising from two different states of confined $NaNO_2$. And eventually the NMR line becomes narrow and Lorentzian when the fraction of the premelted or melted part rises up to 1. Note that the total integral intensity of the ^{23}Na NMR line at high temperatures is larger by a factor of 2.5 than that at low temperatures (Fig. 6) since all spin transitions contribute to the line when $NaNO_2$ is in the melted or premelted state.

The obtained results should be compared with previous studies of confined $NaNO_2$ particles. Until now there were published results of studies of $NaNO_2$ nanoparticles embedded into porous glasses,[36,37] opals,[38] and mesoporous sieves.[39] Using neutron scattering it was shown that the amplitudes of atomic vibration in confined $NaNO_2$ increased remarkably above the bulk ferroelectric phase transition.[36] The authors referred this feature to the whole amount of confined $NaNO_2$ and did not report the simultaneous existence of a bulk-like component. Measurements of sodium spin-lattice relaxation conducted in Ref. 37 were treated as a result of gradual increasing of relaxation rate due to premelting in confined $NaNO_2$. According to Ref. 37, spin relaxation does not show anomalies specific to the ferroelectric phase transition in bulk since premelting involves the whole amount of confined $NaNO_2$. On the other hand, dielectric and NMR studies in Ref. 39 and dielectric studies in Ref. 38 revealed clear anomalies in susceptibility and spin relaxation for $NaNO_2$ embedded into mesoporous sieves and into opals near the bulk ferroelectric phase transition. However, the temperature range of NMR measurements in Ref. 39 was too narrow to allow establishing the coexistence of two states of confined $NaNO_2$ as in the present paper. In contrast to the previous results obtained in Refs. 36–39, we have found the coexistence of ferroelectric and melted (or premelted) states for confined $NaNO_2$ particles. Such a phenomenon is of general interest, especially if one takes into account that gradual melting of fine particles does not destroy ferroelectricity. Mesoporous sieves have some advantages over porous glasses due to much more regular geometry of pore network and narrow pore size distribution. Probably this helped to more clearly separate spin-lattice relaxation into fast and slow parts compared to Ref. 37.

It should be emphasized that the ferroelectric phase transition temperature detected in the present paper for the bulk-like part of confined $NaNO_2$ differs very slightly from that in bulk (Fig. 3). Following warming the samples above the transition, the temperature of the R_{slow} maximum could move relative to the bulk point (Fig. 3 and Ref. 39) but this shift did not exceed 20 K. This result seems rather unexpected, taking into account predictions of theoretical models and studies of isolated small ferroelectric particles[4–7,40–43] according to which the ferroelectric phase transition should be strongly smeared out and moved to low temperatures for nanoparticles within narrow pores of molecular sieves. Possibly, the behavior of the rigid part of confined sodium nitrite is affected by long-distance interaction between particles in adjacent channels.

In conclusion, the results of our NMR studies have shown that sodium nitrite in nanopores occurs in two states which exhibit very different rates of ^{23}Na spin-lattice relaxation. The slow relaxing component corresponds to rigid $NaNO_2$ crystalline lattice which possesses bulk-like properties including the structural phase transition at temperatures near the bulk ferroelectric transition point. Another state exhibits much shorter relaxation times of sodium nuclei corresponding to high molecular mobility as in viscous liquids. The portion of the melted or premelted state of confined $NaNO_2$ increases gradually with increasing temperature and prevails above 510 K in all samples under study. The total amount of melted or premelted $NaNO_2$ at a fixed temperature depends on pore size and geometry and is maximal for $NaNO_2$ within the MCM-41 molecular sieve with 20 Å pore size.

ACKNOWLEDGMENTS

The present work was supported by the National Science Council of Taiwan under Grant No. 93-2811-M-006-021 and by the Deutsche Forschungsgemeinschaft (DFG) and RFBR.

[1] *Ferroelectric Ceramics*, edited by N. Setter and E. L. Colla (Birkhause, Basel, 1993).
[2] I. Yamashita, H. Kawaji, T. Atake, Y. Kuroiwa, and A. Sawada, Phys. Rev. B **68**, 092104 (2003).
[3] R. Böttcher, C. Klimm, D. Michel, H.-C. Semmelhack, G. Völkel, H.-J. Gläsel, and E. Hartmann, Phys. Rev. B **62**, 2085 (2000).
[4] Z. Zhao, V. Buscaglia, M. Viviani, M. T. Buscaglia, L. Mitoseriu, A. Testino, M. Nygren, M. Johnsson, and P. Nanni, Phys. Rev. B **70**, 024107 (2004).
[5] Y. Drezner and S. Berger, J. Appl. Phys. **94**, 6774 (2003).
[6] T. Yu, Z. X. Shen, W. S. Toh, J. M. Xue, and J. Wang, J. Appl. Phys. **94**, 618 (2003).
[7] B. Jiang, J. L. Peng, L. A. Bursill, and W. L. Zhong, J. Appl. Phys. **87**, 3462 (2000).
[8] S. Kohiki, S. Takada, A. Shimizu, K. Yamada, H. Higashijima, and M. Mitome, J. Appl. Phys. **87**, 474 (2000).
[9] Yu. A. Kumzerov and S. B. Vakhrushev, "Nanostructures within porous materials," in *Encyclopedia of Nanoscience and Nanotechnology*, edited. by H. S. Nalwa (American Scientific Publishers, Stevenson Ranch, California, 2003).
[10] H. K. Christenson, J. Phys.: Condens. Matter **13**, R95 (2001).
[11] J. Warnock, D. D. Awschalom, and M. W. Shafer, Phys. Rev. Lett. **57**, 1753 (1986).
[12] E. V. Charnaya, C. Tien, K. J. Lin, and Yu. A. Kumzerov, Phys. Rev. B **58**, 11089 (1998).
[13] Z. W. Liu, Y. Bando, M. Mitome, and J. H. Zhan, Phys. Rev. Lett. **93**, 095504 (2004).
[14] C. Tien, C. S. Wur, K. J. Lin, E. V. Charnaya, and Yu. A. Kumzerov, Phys. Rev. B **61**, 14833 (2000).
[15] M. Larson, N. Mulders, and G. Ahlers, Phys. Rev. Lett. **68**, 3896 (1992).
[16] J. E. Baumgardner and D. D. Osheroff, Phys. Rev. Lett. **93**, 155301 (2004).
[17] V. Krakoviack, Phys. Rev. Lett. **94**, 065703 (2005).
[18] J. Swenson, J. Phys.: Condens. Matter **16**, S5317 (2004).
[19] R. Valiullin and I. Furo, Phys. Rev. E **66**, 031508 (2002).
[20] M. E. Lines and A. M. Glass, *Principles and Applications of Ferroelectrics and Related Materials* (Clarendon Press, Oxford, 2001), Chap. 9.5.
[21] S. Jun, S. H. Joo, R. Ryoo, M. Kruk, M. Jaroniec, Z. Liu, T. Ohsuma, and O. Terasaki, J. Am. Chem. Soc. **122**, 10712 (2000).
[22] J. K. Jung, O. H. Han, and S. H. Choh, Solid State Commun. **110**, 547 (1999).
[23] L. Pandey and D. G. Hughes, J. Phys.: Condens. Matter **4**, 6889 (1992).
[24] N. Okubo, M. Igarashi, and R. Yoshizaki, Z. Naturforsch., A: Phys. Sci. **51A**, 277 (1996).
[25] G. Bonera, F. Borsa, and A. Rigamonti, Phys. Rev. B **2**, 2784 (1970).
[26] T. Gohda, M. Ichikawa, T. Gustafsson, and I. Olovsson, Phys. Rev. B **63**, 014101 (2000).
[27] A. Avogadro, G. Bonera, and A. Rigamonti, J. Magn. Reson. (1969-1992) **20**, 399 (1975).
[28] S. Sen and J. F. Stebbins, Phys. Rev. B **55**, 3512 (1997).
[29] A. Abragam, *Principles of Nuclear Magnetism* (Clarendon Press, Oxford, 1989), Chapt. VIII.
[30] P. S. Hubbard, J. Chem. Phys. **53**, 985 1970.
[31] T. Tokuhiro, J. Magn. Reson. (1969-1992) **76**, 22 (1988).
[32] S. H. Choh, J. Lee, and K. H. Kang, Ferroelectrics **36**, 297 (1981).
[33] V. Lyahovitskaya, Y. Feldman, I. Zon, E. Wachtel, K. Gartsman, A. K. Tagantsev, and I. Lubomirsky, Phys. Rev. B **71**, 094209 (2005).
[34] P. Porion, M. P. Faugere, E. Lecolier, B. Gherardi, and A. Delville, J. Phys. Chem. **102**, 3477 (1998).
[35] Y. Inagaki, H. Maekawa, T. Yokokawa, and S. Shimokawa, Phys. Rev. B **47**, 674 (1993).
[36] A. V. Fokin, Yu. A. Kumzerov, N. M. Okuneva, A. A. Naberezhnov, S. B. Vakhrushev, I. V. Golosovsky, and A. I. Kurbakov, Phys. Rev. Lett. **89**, 175503 (2002).
[37] S. B. Vakhrushev, Yu. A. Kumzerov, A. Fokin, A. A. Naberezhnov, B. Zalar, A. Lebar, and R. Blinc, Phys. Rev. B **70**, 132102 (2004).
[38] S. V. Pankova, V. V. Poborchii, and V. G. Solovev. J. Phys.: Condens. Matter **8**, L203 (1996).
[39] C. Tien, E. V. Charnaya, S. V. Baryshnikov, M. K. Lee, S. Y. Sun, D. Michel, and W. Böhlmann, Phys. Solid State **46**, 2301 (2004).
[40] W. L. Zhong, Y. G. Wang, P. L. Zhang, and B. D. Qu, Phys. Rev. B **50**, 698 (1994).
[41] B. Jiang and L. A. Bursill, Phys. Rev. B **60**, 9978 (1999).
[42] Y. G. Wang, W. L. Zhong, and P. L. Zhang, Phys. Rev. B **53**, 11439 (1996).
[43] E. V. Charnaya, O. S. Pogorelova, and C. Tien, Physica B **305**, 97 (2001).